

# A constrained iteratively-reweighted least-squares framework for generalised linear models

Pierre Masselot<sup>1</sup>, Devon Nemon<sup>1</sup>, Jacopo Vanoli<sup>2</sup>, Zaid Chalabi<sup>3</sup>, Antonio Gasparri<sup>1</sup>

<sup>1</sup>*Environment & Health Modelling (EHM) Lab, Department of Public Health, Environment & Society, London School of Hygiene & Tropical Medicine, London, UK*

<sup>2</sup>*Institute of Social and Preventive Medicine (ISPM), University of Bern, Bern, Switzerland*

<sup>3</sup>*UCL Institute for Environmental Design and Engineering, The Bartlett School of Environment, Energy and Resources, University College London, London, UK*

## Abstract

Many applications of generalised linear models (GLMs) can be improved by applying constraints that impose assumptions on the associations or improve consistency of the estimators. Yet, there are still barriers to the implementation and practical application of constrained GLMs. We present a general framework for fitting GLMs subject to linear constraints on the coefficients that offers original and interesting features. First, estimation is performed using constrained iteratively-reweighted least-squares (CIRLS), offering fast and stable algorithms with excellent convergence performance. Second, the development includes advanced inferential procedures based on truncated multivariate normal distribution and corrected degrees of freedom that account for the constrained nature of the estimation problem. Extensive simulation studies indicate good inferential and computational properties, even in the case of slightly overconstrained models. Third, the proposed methods are fully implemented in the ‘cirls’ library for the R software, embedding constrained estimation in standard regression routines with simple usage and syntax. Two real-data case studies provide examples of applications for constrained dose-response estimation and compositional data analysis. The CIRLS framework and software offer a unified approach for various constrained estimation problems across a wide range of research areas.

## Introduction

Generalised linear models (GLM) are ubiquitous in statistics, being used in virtually every quantitative scientific field. GLMs model the association between a linear predictor and many different types of outcomes, including continuous, binary and count variables, through a link function that impose a shape to this association. GLM modelling now consists of an established framework that also includes a comprehensive set of methods for inference, model selection, and diagnostics (Dobson and Barnett, 2018).

There are situations in which it is useful to impose constraints on the coefficients of a GLM. Such constraints can represent specific assumptions or prior knowledge on the estimated associations, restricting unrealistic estimates or simply improving the fit. Many of the most commonly encountered constraints can be expressed as a set of linear combinations of the coefficients, especially when applying specific parametrisations to the predictors, for instance for shape or order constraints, (Silvapulle and Sen, 2005) or constraints for variables that are relative to a reference (Altenbuchinger et al., 2017). However, despite the usefulness of linear constraints in GLMs, there is generally no established framework that offers comprehensive methods for the various steps involving estimation, inference, and model selection. Previous work on fitting algorithms (Hofner et al., 2016; Meyer, 2013a; Zhou and Lange, 2013) and inference (Davis, 1978; Geweke, 1996) is mostly limited to linear models, with extensions to GLMs remaining sparse. These limitations are compounded by the lack of software implementation, putting practical barriers to the application of constrained GLMs.

In this contribution, we propose a flexible framework for GLMs subject to linear constraints on the coefficients, providing standardised procedures for their applications. The centrepiece of this framework is the constrained iteratively-reweighted least-squares (CIRLS) fitting algorithm, which exploits the speed and efficiency of quadratic programming (Goldfarb and Idnani, 1983). It quickly converges towards the solution, overcoming computational barriers to the practical application of constrained GLMs. Once a model is fitted, inference for the constrained coefficients can be performed through a truncated multivariate normal (TMVN) distribution (Horrace, 2005) from which confidence and prediction intervals can be obtained. We also account for the reduced effective complexity of constrained models, with a procedure to estimate their expected degrees of freedom that can typically be used with a  $C_p$  or Akaike Information Criterion (AIC) estimate of prediction error (Akaike, 1974; Mallows, 1973). The full framework is implemented in the `cirls` package for the R software (Masselot and Gasparrini, 2025), providing efficient routines and easy-to-use syntax to fit various types of constrained models.

The CIRLS framework can be used to fit a wide range of different models, allowing for many different practical applications. An example is monotonic regression including non-parametric regression and splines, as shown in the first application where we estimate the rate of global temperature increase since 1850. Another example is compositional regression, where some predictors represent relative quantities and sum to a constant (Aitchison and Bacon-Shone, 1984). In this context, we use the CIRLS framework to estimate how relative expenditure in European countries is associated with their life expectancy (Hron et al., 2012). Beyond these two examples, the CIRLS framework can be generally used to define any type of constrained model, such as cone regression (Meyer, 2013a), shape-constrained splines (Meyer, 2018; Pya and Wood, 2015), ordinal models (Espinosa and Hennig, 2019), simplicial-simplicial regression (Tsagris, 2025) as well as the Lasso and many of its extensions (Gaines et al., 2018; Tibshirani, 1996).

The remainder of the paper is organised as follows. A first section introduces the modelling framework and the CIRLS algorithm followed. It is followed by the related analytical framework, which includes the distribution of constrained coefficients and effective degrees of freedom. The next section reports the results of extensive simulation studies, assessing the statistical and inferential properties of the framework. The framework is then illustrated in two real-world case studies, while a final section provides a discussion.

## The Constrained Iteratively-Reweighted Least-Squares algorithm

### *Constrained Generalised Linear Models*

The objective is to estimate the following GLM with linearly constrained coefficients

$$\begin{aligned} g(\mu_i) &= \mathbf{x}_i^T \boldsymbol{\beta} \\ \text{subject to} \quad & \mathbf{l} \leq \mathbf{C}\boldsymbol{\beta} \leq \mathbf{u} \end{aligned} \quad (1)$$

where  $\mu_i = \mathbb{E}(y_i)$  and  $y_i$  ( $i = 1, \dots, n$ ) is a response variable assumed to follow a distribution from the exponential family with a monotonic link function  $g(\cdot)$  (McCullagh and Nelder, 1989).  $\mathbf{x}_i$  is a vector of  $p$  predictors and  $\boldsymbol{\beta}$  the associated  $p$ -dimensional vector of coefficients. In a constrained GLM, we assume that the vector of coefficients  $\boldsymbol{\beta}$  is subject to  $m$  linear constraints encoded by a  $m \times p$  constraint matrix  $\mathbf{C}$  with lower and upper bound  $m$ -dimensional vectors  $\mathbf{l}$  and  $\mathbf{u}$ .

The definition in (1) encompasses all types of constraints mentioned in the introduction. For instance, non-negative GLMs can be specified by setting  $\mathbf{C} = \mathbf{I}_m$ , with  $\mathbf{I}_m$  as an identity matrix,  $\mathbf{l}$  is an  $m$ -dimensional vector of zeros, and  $\mathbf{u} = +\infty$ . Compositional regression can be specified with  $\mathbf{C} = \mathbf{1}_m^T$  (a vector of ones) and  $\mathbf{l} = \mathbf{u} = 0$ , while in the Lasso  $\mathbf{C}$  includes  $2^p$  rows that represent all possible combinations of non-null coefficients and  $\mathbf{l}$  is a vector of zeros and  $\mathbf{u} = t$  (although it can be simplified, Gaines et al., 2018). Additional examples are provided in the simulation study and applications below. In all cases, only a subset of predictors in  $\mathbf{x}_i$  can be constrained, in which case  $\mathbf{C}$  is padded with zeros for the unconstrained variables.

### *Constrained Iterative Reweighted Least Squares*

The unconstrained GLM is usually fitted with iteratively-reweighted least-squares (IRLS) algorithm where, at each iteration, the estimated  $\boldsymbol{\beta}$  is updated by minimising

$$\begin{aligned} \hat{\boldsymbol{\beta}}^{[k+1]} &= \min_{\boldsymbol{\beta}} \sum_i w_i (z_i - \mathbf{x}_i \boldsymbol{\beta})^2 \\ &= \min_{\boldsymbol{\beta}} (\mathbf{z} - \mathbf{X}\boldsymbol{\beta})^T \mathbf{W} (\mathbf{z} - \mathbf{X}\boldsymbol{\beta}) \end{aligned} \quad (2)$$

with  $\mathbf{X}$  a  $n \times p$  matrix that includes  $\mathbf{x}_i'$  as its  $i^{\text{th}}$  row. In Equation (2),  $\mathbf{z}$  is a pseudo-response vector and  $\mathbf{W}$  a diagonal pseudo-weights matrix.  $\mathbf{z}$  and  $\mathbf{W}$  depend on the current iteration of  $\hat{\boldsymbol{\beta}}^{[k]}$  and on the specific distribution of  $y_i$ , with their full expression covered extensively elsewhere (McCullagh and Nelder, 1989; Wood, 2017). The minimisation problem in Equation (2) is iterated until convergence, *e.g.* until the decrease in deviance remains below a predefined small threshold.

In the extension to the constrained iteratively-reweighted least-squares (CIRLS) algorithm, we subject each step of the algorithm (2) to the constraints of Equation (1) so that each update  $\hat{\boldsymbol{\beta}}^{[k]}$  remains feasible. Rearranging the least-squares function of (2), we have the following constrained optimisation problem

$$\hat{\boldsymbol{\beta}}^{[k+1]} = \min_{\boldsymbol{\beta}} (\boldsymbol{\beta}^T \mathbf{X}^T \mathbf{W} \mathbf{X} \boldsymbol{\beta} - 2\mathbf{z}^T \mathbf{W} \mathbf{X} \boldsymbol{\beta} + \mathbf{z}^T \mathbf{z}) \quad (3)$$

$$\text{s. t. } \mathbf{l} \leq \mathbf{C} \boldsymbol{\beta} \leq \mathbf{u}$$

The CIRLS step, as laid out in Equation (3), is a typical Quadratic Program (QP) for which many efficient algorithms exist (Boyd and Vandenberghe, 2004). In the simulations and applications below, the QP in (3) will be solved by a dual algorithm (Goldfarb and Idnani, 1983), but other equally efficient algorithms can be considered, such as the alternating direction method of multipliers (Stellato et al., 2020), or cone projection (Meyer, 2013a).

Another way to view the CIRLS algorithm is as a Sequential Quadratic Program (SQP). These algorithms are useful to solve general nonlinear constrained optimisation problems and, under some conditions that are generally met in the specific case of constrained GLMs, tend to converge quickly (Boggs and Tolle, 1995). Appendix 1 provides additional details on this connection between CIRLS and SQP.

## Inference

When regression is fitted with constraints, the usual asymptotic theory providing distributions and inference for the coefficients is no longer valid (Wets, 1991). Indeed, the application of typical formulas results in probability distributions that can include unfeasible coefficient vectors, *i.e.* coefficients that violate the constraints in (1). In this section, we describe inference for coefficients estimated by CIRLS and model selection for the constrained GLM.

### *Distribution*

In unconstrained models, the estimated coefficient vector  $\hat{\boldsymbol{\beta}}$  is asymptotically multivariate Gaussian (Wood, 2017). Truncating such a distribution has been a longstanding topic of analysis (Tallis, 1965) and the resulting TMVN is nowadays well characterised (Horrace, 2005). More specifically to constrained GLMs, it can be shown that the linearly transformed coefficient vector  $\mathbf{C}\hat{\boldsymbol{\beta}}$  follows a TMVN (Geweke, 1996), *i.e.* we have that

$$\mathbf{C}\hat{\boldsymbol{\beta}} \sim \text{TMVN}(\mathbf{C}\boldsymbol{\beta}^*, \phi^* \mathbf{C} \mathbf{X}^T \mathbf{W}^* \mathbf{X} \mathbf{C}^T, \mathbf{l}, \mathbf{u}) \quad (4)$$

where  $\boldsymbol{\beta}^*$ ,  $\mathbf{W}^*$ , and  $\phi^*$  are respectively the coefficient vector, weight matrix, and dispersion parameters from an *unconstrained* model. Note that the distribution in (4) is also found from a Bayesian perspective using a typical uninformative prior multiplied by an indicator function assigning null probability mass to unfeasible coefficient vectors (Davis, 1978; Geweke, 1986; Ghosal and Ghosh, 2022).

There has been some work exploring the properties of TMVN distributions (Horrace, 2005), proposing formulas for the moment generating function (Tallis, 1965, 1961) and from there the first and second moments (Kan and Robotti, 2017; Manjunath and Wilhelm, 2021). However, these formulas do not allow the computation of, *e.g.*, confidence intervals, and their evaluation can be difficult when the number of coefficients increases. It is instead more flexible to simulate from (4), transform back to obtain realisations of  $\boldsymbol{\beta}$ , and compute the desired summaries from there. This can be performed for any number of constraints up to  $p$ , with computational details provided in Appendix 2. In this paper, we simulate from (4) using the scheme of Botev (2017), which uses exponential tilting in an importance sampling scheme to address acceptance rate issues from previous algorithms (Geweke, 1991). This approach is efficient even for high-dimensional vectors and is implemented in the R software (Botev et al., 2024).

From the distribution in (4), it can be shown that  $\mathbb{E}(\mathbf{C}\hat{\boldsymbol{\beta}}) \neq \mathbf{C}\boldsymbol{\beta}^*$  even when  $\boldsymbol{\beta}^*$  would be feasible, *i.e.* that the constrained estimator is biased. On the other hand, the constrained estimator has reduced variance compared to the unconstrained one (Barr and Sherrill, 1999; Liew, 1976), as discussed in Appendix 2. This suggests a trade-off between increased bias and reduced variance due to the constraints, which can be advantageous in terms of estimation error. This property is explored in the simulation study below.

### Degrees of freedom

Characterising degrees of freedom for a model is useful for residual variance estimation or for use in model selection criteria, such as the Akaike Information Criterion (AIC) or Bayesian Information Criterion (BIC) (Burnham and Anderson, 2004). When constraints are applied, degrees of freedom are reduced due to the restrictions imposed to the coefficients. For instance, in the Lasso, degrees of freedom can be shown to be equal to the number of non-zero coefficients (Efron et al., 2004), while in isotonic regression it corresponds to the number of distinct predictions (Meyer and Woodroffe, 2000). More generally, for any linearly constrained model, the degrees of freedom are

$$odf = p - m_a \quad (5)$$

where  $p$  is the number of parameters in the model and  $m_a \in \{0, \dots, m\}$  is the number of active constraints in the fitted model. A constraint represented by the row  $\mathbf{c}_i$  ( $i = 1, \dots, m$ ) is active when  $\mathbf{c}_i\hat{\boldsymbol{\beta}} = l_i$  or  $\mathbf{c}_i\hat{\boldsymbol{\beta}} = u_i$ , *i.e.* when an unconstrained model would have yielded an unfeasible solution with respect to the  $i^{th}$  constraint.

We refer to (5) as *observed* degrees of freedom because the value of  $m_a$  depends on samples  $y_i$ , and the number of degrees of freedom can be considered a random variable taking values from  $p - m$  to  $p$  (Meyer, 2013b). Therefore, *odf* might overstate the reduction in degrees of freedom induced by the constraints, which can be damaging, in particular for model selection. For instance, a predictor  $x_{ij}$  that is uncorrelated with  $y_i$  has an actual coefficient that is null, which means that it is likely the nonnegativity constraint associated with this variable would be active. In this case, the added complexity from this additional variable is not represented in *odf*, and any model selection using it would tend to favour overly complex models.

To better represent the complexity of a model, we also consider *expected* degrees of freedom as (Meyer, 2013b):

$$edf = p - \sum_{k=0}^m k\mathbb{P}(m_a = k) \quad (6)$$

The term  $\sum_{k=0}^m k\mathbb{P}(m_a = k)$  represents the expected number of active constraints for the model defined in (1), with the weight  $\mathbb{P}(m_a = k)$  being the probability of having exactly  $k$  active constraints. These weights can be estimated by simulating from a multivariate normal distribution of the unconstrained coefficients, counting the number of constraints that would be active in each instance. Here we use the terms *observed* and *expected* degrees of freedom, instead of the generally used *effective* degrees of freedom, to clearly differentiate degrees of freedom computed by (5) and (6).

## Practical implementation: the R package ‘cirls’

To make the framework as convenient to use as possible in practice, we provide an R implementation of the framework in R through the package ‘cirls’ (Masselot and Gasparrini, 2025). It provides a `cirls.fit()` function that embeds the CIRLS algorithm in the standard function `glm()`. The user can then implement various models using a simple syntax, exploiting various

features of the standard R implementation for GLM. This implementation includes the possibility to use several different QP algorithms (Goldfarb and Idnani, 1983; Meyer, 2013a; Stellato et al., 2020), offering fast and reliable routines with good convergence performances. The package implements inference and model selection through specific methods for standard functions such as `vCOV()`, `confint()`, and `logLik()`. This can be combined with other usual functions like `AIC()` and `BIC()`.

The package has also been developed for flexibility, providing different interfaces for constraint specification, all complementing each other. Common constraints can easily be provided through a formula interface, while more complex constraint matrices can also be passed directly. These interfaces allow the expansion of the package via user-written interface functions. These interfaces are used in the simulations and practical applications below, as shown in the reproducible code attached to this paper.

## Simulation study

In this section, we evaluate the properties of the CIRLS framework introduced in this paper, including the estimation error of the coefficients  $\beta$ , the accuracy of the inference, and the definition of expected degrees of freedom exposed above.

### *General strategy*

We consider two applications of constrained GLM: i) a non-negative regression; and ii) a non-decreasing regression of population means. In each application, the data-generating mechanism (DGM) is defined by a linear predictor  $\eta(x_i)$  that sets the true association between  $x_i$  and  $y_i$ , and the distribution of  $y_i$ . The linear predictor  $\eta(x_i)$  depends on a *feasibility* parameter  $\gamma$  controlling how feasible  $\eta(x_i)$  is, related to the constraints of the specific application. The parameter  $\gamma$  varies from -1 (unfeasible) to 1 (feasible), with 0 corresponding to the boundary of the feasible region. From each DGM, we simulate  $n_{sim} = 1000$  datasets of  $n = 500$  observation, with the distribution of  $y_i$  set to result in a low signal-to-noise ratio. These DGMs are meant to emulate a low-power setting as a realistic real-world situation in which constraints would typically be useful. All the parameters of data-generating mechanisms are shown in Table 1.

Estimation performances of the CIRLS fit are evaluated by computing the Bias, Standard Error (SE) and Root Mean-Squared Error (RMSE). These three performance measures are computed on a constrained and an unconstrained fit, and we then show the difference between the two. Inference is evaluated by computing the relative error of coefficient variance as well as 95% confidence intervals coverage. Finally, our degrees of freedom formulae (5 and 6) are compared to the true degrees of freedom computed from the simulations (Shen et al., 2004; Ye, 1998). The specific formulae for all these performance criteria can be found in Appendix 3 (equations 11 and 12).

### *Data-generating mechanisms*

The first DGM emulates a simple non-negative least-squares problem in which the coefficient associated with a variable of interest is assumed to be positive or null. Two correlated standard normal predictors (with correlation  $\rho = 0.5$ ) are generated, and the linear predictor is defined as

$$y_i = \eta(x_i) = 5 + \beta_1 x_{i1} + \beta_2 x_{i2} + \epsilon_i \quad (7)$$

where  $\epsilon_i$  follows a centred normal distribution with  $\sigma^2 = 50$  to emulate a low power setting. Here, the feasibility parameter is simply the main coefficient of interest  $\gamma = \beta_1$ , which varies between -1

and 1.  $\beta_2 = 1$  is the “covariate” coefficient, which does not vary in the DGM. In this setting, we therefore have  $\mathbf{C} = [0 \ 1 \ 0]$  with  $l = 0$  and  $u = +\infty$ .

The second DGM emulates estimation of population subgroup characteristics in which a monotonicity assumption is made. This is typically encountered in stratified surveys, for instance (Oliva-Aviles et al., 2019). Here, a single categorical predictor  $x_i$  is generated from a discrete uniform distribution with 5 levels. The linear predictor is defined as

$$\eta(x_i) = \frac{\gamma}{1 + \exp(-50x_i)} \quad (8)$$

which is a logistic function with a relatively small amplitude to result in low counts. The response  $y_i$  is then generated as a Poisson variable with rate  $\exp(\eta(x_i))$ . The feasibility parameter varies from  $-1$  (in which case  $\eta(x_i)$  decreases with the level of  $x_i$  and thus violates the constraints) to  $1$  (in which case  $\eta(x_i)$  increases). When  $\gamma = 0$ , then  $\eta(x_i)$  is constant. Here, the predictor  $x_i$  is expanded into dummy variables, and we have a  $4 \times 5$   $\mathbf{C}$  matrix such that  $c_{ii} = 1$ , and  $c_{ij} = -1$  when  $j = i + 1$  and zero elsewhere, with  $\mathbf{l}$  and  $\mathbf{u}$  four-dimensional vectors of zeros and  $+\infty$  respectively. The two DGMs are summarised in Table 1 and illustrated in Appendix 3.

## Results

### Estimation error

Figure 1 shows the estimation performances of a constrained model relative to an unconstrained one for various values of the feasibility parameter  $\gamma$ . In both DGM and for all coefficients, there is a clear decreasing trend in Bias and an increase in the Standard error, both converging towards zero, (*i.e.*, their values in the unconstrained model) when increasing the feasibility parameter  $\gamma$ . This results in inverse-J shaped curves of RMSE, where the RMSE is high for the constrained model for widely unfeasible linear predictors, then decreases with the bias to become negative (*i.e.*, improving upon the unconstrained model), to then increase again with Standard error to converge towards zero. This pattern is observed in all reported coefficients in Figure 1, but with various amplitudes. In the first DGM, the RMSE of the ‘covariate’ coefficient displays this pattern but with a lower amplitude than the main coefficient. In the second DGM, strata 1 and 5 are more sensitive to the constraints being well defined, with the bias and RMSE increasing rapidly when  $\gamma$  decreases.

Interestingly, the improvement in RMSE also happens for several negative feasibility parameters, *i.e.* in which the true linear predictor is actually slightly outside of the feasible region. In the first DGM, for instance, the RMSE difference is negative even for a true coefficient  $\beta_1 = -0.3$ , while it is negative in almost all situations for Strata 3 in the second DGM. The lowest value of RMSE is generally close to the boundary of the feasible region, which outlines the importance of carefully choosing the constraints. But overall, constraints, even slightly wrong ones, can be beneficial for the estimation performances of a GLM.

### Uncertainty assessment

Figure 2 shows the error in inference procedures according to the feasibility  $\gamma$  of the linear predictor. In both DGMs, the variance is overestimated when the true linear predictor is unfeasible, and slightly underestimated for feasible models, with the amplitude of the error depending on how constrained the coefficient is. However, except for the main coefficient of the first DGM when  $\gamma$  is low, the error remains within 30%. The error is often negligible when the true linear predictor is near the boundary of the feasible region ( $\gamma = 0$ ).

Similarly, the coverage is null when the coefficients are not feasible since, by definition, it cannot include the true coefficient value. In the first DGM (bottom left panel), for the lowest feasibility parameter, this also brings the coverage of the covariate coefficient down due to the added bias (Figure 1a). However, when feasible, the coefficient immediately reaches 95% coverage with a slight over-coverage for the feasibility parameter between  $\gamma = 0.2$  and  $\gamma = 0.6$ . In the second DGM (bottom right panel), the same pattern is visible, although smoother since the constraints are not directly on the coefficient value but on their relation. The middle strata coefficient reaches the 95% level even in slightly unfeasible cases, while on the other hand, the lower and middle strata coefficients close on the 95% value for the highest values of  $\gamma$ . Note that, when correcting for the bias, the coverage is close to the nominal level even for some over-constrained models, indicating an acceptable confidence interval width (see appendix 3).

### Degrees of freedom

Figure 3 shows the RMSE between both *odf* and *edf*, and the actual degrees of freedom computed from the simulated observations. It indicates that *edf* tends to be a better estimate of model complexity than *odf* for feasible models, as well as unfeasible ones that are close to the boundary. The difference is much more important in the second DGM where several constraints are involved than in the first DGM, suggesting the usefulness of *edf* might increase with more complex constraints. Note that *odf* is generally unbiased but unstable since it ignores the randomness in the number of active constraints. *edf*, that accounts for randomness, has much lower standard error, especially close to the boundary between feasible and unfeasible models, but at the cost of some bias, especially for widely over-constrained models (see appendix 3).

## Real-world case studies

### *Global temperature anomaly*

In this first example, we use the CIRLS framework to estimate the rate of global warming increase between 1850 and 2015, using a dataset of global temperature anomalies compared to the period 1961-1990 provided by Jones et al. (2000). We first want to detect change-point periods, which can be framed as a monotone regression problem assuming a non-decreasing trend (Alvarez and Dey, 2009; Wu et al., 2001). Therefore, we fit a model of global temperature anomaly with an ordinal predictor that represents five-year periods. The constraint matrix encodes a non-decreasing function of strata, which includes  $p - 1$  constraints  $\beta_{j+1} - \beta_j \geq 0$  with  $p = 34$  as the number of periods of five years spanned by the data.

The resulting estimate is shown in Figure 4a along with an unconstrained model for comparison. During stable periods, the constrained model stabilises the fit compared to the unconstrained one, while they correspond almost perfectly in periods of strong temperature increase, i.e. 1910-1940 and even stronger temperature increase since 1970. Notice that the confidence band shifts upwards even when the point estimate is constant, reflecting the non-decreasing constraint on the levels. In this application, *odf* indicates the number of changepoints, here being equal to 17 out of the 34 periods, while *edf* estimates about 22 expected change-points.

To go further, we now seek to estimate a smooth function of global warming which we do through non-decreasing splines. More specifically, we expand the year through a natural spline basis with ten degrees of freedom, on which we impose non-decreasing coefficients, which is sufficient to enforce the shape constraint (Pya and Wood, 2015). The result is shown in Figure 4b with a very similar shape to the strata model and illustrates that the non-decreasing constraint regularises the fit to obtain a smoother function than the unconstrained one. This is outlined by expected degrees of

freedom that are here estimated to 8.6 for this model, compared to the 12 degrees of freedom of the unconstrained model (ten for splines with the addition of the intercept and the dispersion parameter).

### *GDP composition and life expectancy*

In this second case study, we use data provided by Hron and colleagues (2012) that report the life expectancy of the 27 European Union member states for men and women along with their Gross Domestic Product (GDP) broken down into six categories: (i) agriculture, hunting, forestry and fishing, (ii) mining and manufacturing, (iii) construction, (iv) wholesale, retail, restaurant and hotels, (v) transport storage and communication, and (vi) other activities including health and education. The objective is to assess how the proportion of each category impacts life expectancy, which is a typical compositional regression problem (Aitchison and Bacon-Shone, 1984). In the CIRLS framework, it can be fitted by using  $x_{ij} = \log(z_{ij})$  where  $z_{ij}$  is the relative proportion of category  $j$  for country  $i$ , with the constraint that  $\sum_j \beta_j = 0$  (Aitchison and Bacon-Shone, 1984). This equality constraint ensures that changes in some components  $x_{ij}$  are balanced by opposite changes in other components  $x_{ij'}$  thus following the nature of compositions. Here, we additionally include total GDP as a covariate since it is associated with life expectancy and can be correlated with the proportion of specific categories. Therefore, the constraint matrix is  $\mathbf{C} = [0 \quad \mathbf{1}_6 \quad 0]$ , with  $\mathbf{1}_6$  as a six-dimensional vector of ones, and the bounds are  $l = u = 0$ . The two zeros in  $\mathbf{C}$  indicate the absence of constraints imposed on the intercept and the total GDP.

Estimated coefficients for the GDP components are displayed in Figure 5, showing they indeed sum to zero for both men and women. The results suggest a lower life expectancy in countries with a higher proportion of GDP dedicated to transport and communication, but an increase in life expectancy related to the ‘Other’ category, which likely reflects the effect of services such as education and public health (Hron et al., 2012). Fitting such a model within the constrained GLM framework makes the results easier to interpret compared to approaches based on log-ratio, as it doesn’t depend on the choice of a reference variable (Shi et al., 2016). Additionally, it would be easy to add other constraints if, for instance, we assume the effect of total GDP on life expectancy is necessarily non-negative.

## Discussion

In this contribution, we developed constrained iteratively-reweighted least-squares (CIRLS) to estimate GLMs with constrained coefficients. We also discuss the distribution of constrained coefficients for inference and the representation of the model’s complexity through its degrees of freedom. Our simulation study suggests that appropriately defined constraints improve the accuracy of coefficient estimation through decreased estimation variance, despite the introduction of a slight bias. Importantly, this property was also observed when constraints excluded the true generated coefficients to a certain extent. Two case studies apply CIRLS for monotonic regression and compositional regression, illustrating its flexibility in various settings. Although dedicated solutions exist for either problem (Busing, 2022; Hron et al., 2012), the CIRLS algorithm allows the integration of both, as well as many others, within the same framework, making it easy to perform a wide range of applications.

To make the application of constrained GLMs with CIRLS more accessible, we have developed an R package ‘cirls’ that implements the methods in the paper. This package plugs in the familiar ‘glm’ machinery in R, allowing the use of well-known methods for results interpretation and dissemination. We have also included dedicated methods for inference and model selection, where

the constrained context would cause the classical methods to fail. Finally, we provide a range of convenience functions to build the matrix  $\mathbf{C}$  for common types of constraints, such as sum-to-zero constraints for compositional and relative predictors (Altenbuchinger et al., 2017; Shi et al., 2016), or difference constraints for shape-constrained splines (Meyer, 2008; Pya and Wood, 2015).

Experiments with the CIRLS algorithm for this paper have shown that the CIRLS algorithm converges quickly. CIRLS can be shown to be a Sequential Quadratic Program (SQP), a general class of algorithms that can solve nonlinear constrained optimisation problems rather efficiently (Boggs and Tolle, 1995). Some work has shown that such algorithms converge quadratically to a local optimum (Nocedal and Wright, 2006) under some conditions that are broadly met in the constrained GLM context. In CIRLS, each step of the algorithm uses highly efficient algorithms to solve quadratic programs (Goldfarb and Idrani, 1983; Stellato et al., 2020), ensuring a low computational burden. We refer the reader to Appendix 1, which develops this point further.

We have proposed a framework for the inference of coefficients drawing from TMVN distributions, which showed acceptable properties in our simulations. However, this framework presents important limitations which can hamper inference in many practical applications. First, the framework limits inference to applications where the number of constraints  $m$  is no larger than the number of variables  $p$ , otherwise the inverse transformation cannot be computed. Although this allows many practical cases, this prevents inference in some useful applications, such as S-shaped regression (Meyer, 1999) or the Lasso (Tibshirani, 1996). In the  $m > p$  case, it is possible to combine the proposed inference with an accept-reject algorithm in which the TMVN sampling is performed with a selection of  $p$  constraints, and retains only the samples that satisfy the remaining  $m - p$  constraints (Geweke, 1996). However, the practicality of this approach depends on the acceptance rate, which can be prohibitively low when  $m - p$  is high.

Another limitation of the inference approach is that it necessitates fitting the equivalent unconstrained model used in (4). This typically precludes inference in  $p \geq n$  applications in which the constrained GLM can be fitted but the unconstrained cannot, which includes the Lasso as well as isotonic regression as performed in the first case study. Previous works have proposed inference for individual coefficients for the Lasso and variable selection more generally (Lee et al., 2016; Taylor and Tibshirani, 2015). It takes advantage of the result that the distribution of individual coefficients, conditional on other coefficients, is a truncated univariate normal (Horrace, 2005). Although this requires more complex formulas than what is proposed in the present paper, these results can represent a way forward to generalise the inference from CIRLS fits.

The Bootstrap can represent a flexible alternative for inference in the more extreme applications of CIRLS as described above. It has been used extensively for the Lasso (Hastie et al., 2015), other constrained regression models (Masselot et al., 2023), as well as for the estimation of the mixture probabilities in degrees of freedom computation (Meyer, 2013b). However, it is more computationally demanding, and its application is less trivial in constrained estimation. Parametric Bootstrap, as used in other applications (Meyer, 2003), can only be performed when the unconstrained model can be fitted. Additionally, the Bootstrap generally tends to be inconsistent for inference when parameters are close to the boundary of their feasible space (Andrews, 2000) and therefore require more complex procedures (Li, 2025).

Future work must focus on the extension of inference to hypothesis testing. In many applications, there is interest in testing how binding the constraints are and whether they represent good assumptions on the relationship. Examples include testing the positivity of coefficients (Davis, 1978) and the shape of a nonlinear association (Meyer, 2003; Sen and Meyer, 2017). Additionally, it is of

interest to provide significance tests for coefficients in the presence of constraints. Finally, future work can expand the applicability of CIRLS, allowing nonlinear constraints, including, for instance, Ridge-type constraints useful for smoothing coefficients. The algorithm can also be extended to non-exponential likelihoods such as the negative binomial or Cox proportional hazard models. Both potential extensions can make use of more general SQP algorithms.

In conclusion, the CIRLS algorithm represents a simple and flexible framework for GLMs with linear constraints on the coefficients. Such constraints can help the analysis of biomedical or epidemiological data in situations in which a classical GLM would be difficult to fit, with clear improvements on the estimation of coefficients when the constraints are appropriately set. The proposed inference and degrees of freedom allow the analyst to perform the usual tasks of model selection and confidence interval computation.

## Acknowledgements

This research is supported by the Medical Research Council (MRC) of the United Kingdom (grant MR/X029476/1).

## Data and code

The methods proposed in this paper are implemented in the package ``cirls`` for the open-source software R. The simulation study and illustrative applications can be fully replicated, with R code and data available on GitHub (<https://github.com/PierreMasselot/CIRLS-GLM>).

## Tables

Table 1. Description of the two data-generating mechanism (DGM) for the simulation study. The first three columns indicate how the data are generated, while the last two indicate the corresponding fitted constrained GLM. “Coefficient estimators” indicate the quantity each GLM is attempting to estimate.

Data-generating mechanism	$x_i$	$\eta(x_i)$	$y_i$	Coefficient estimators	CIRLS constraints
Non-negative regression	$MVN(0, \Sigma)$ with $\Sigma_{ii} = 1$ and $\Sigma_{ij} = 0.5$ when $i \neq j$ .	$5 + \gamma X_1 + X_2$	$N(\eta(x_i), 50)$	$\beta_1 = \gamma$ $\beta_2 = 1$	$\beta_1 \geq 0$
Non-decreasing strata	$unif\{1, \dots, 5\}$	$\frac{\gamma}{1 + \exp(-50x_i)}$	$Poisson(\exp(\eta(x_i)))$	$\beta_j = \eta(j)$	$\beta_{j+1} - \beta_j \geq 0$

## Figure captions

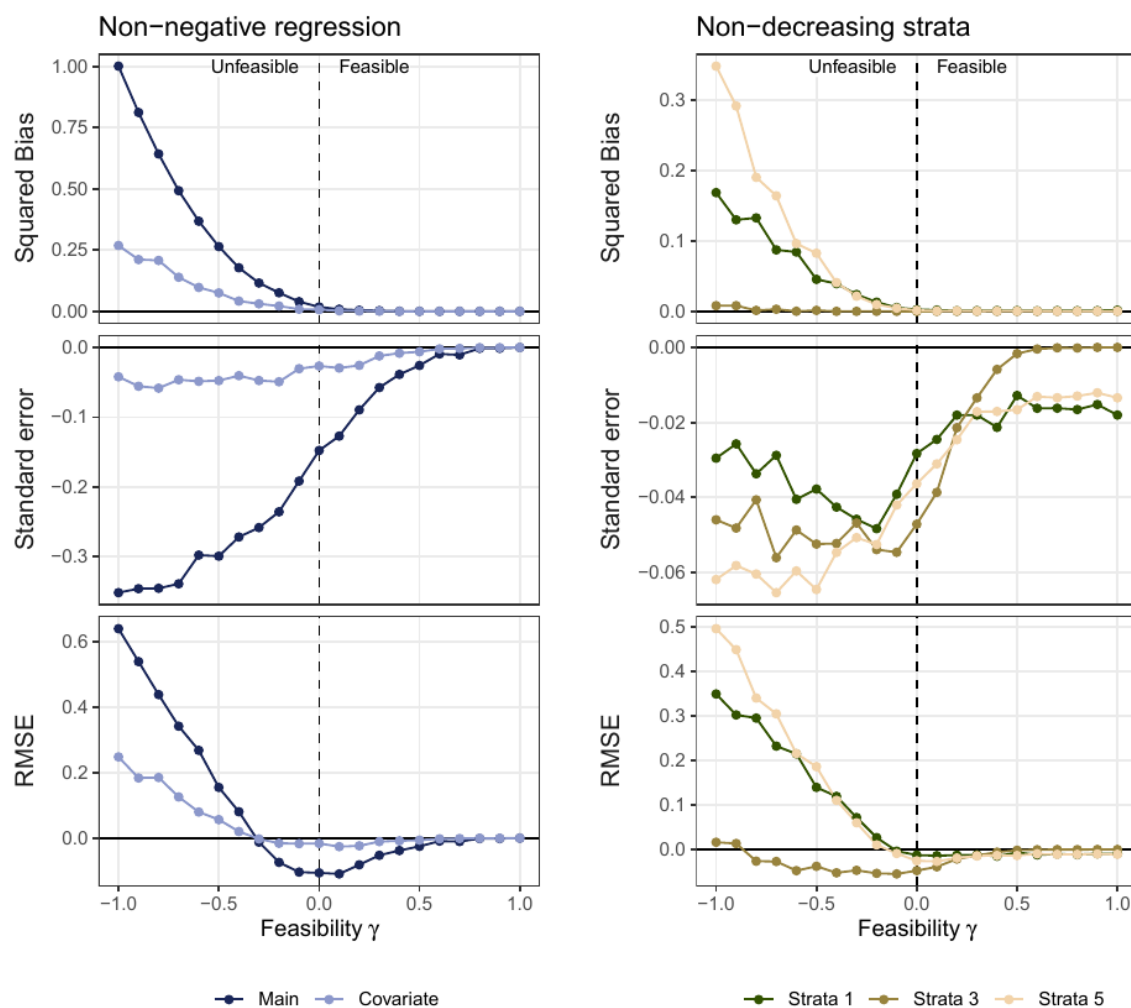


Figure 1. Increase in squared Bias, Standard error and Root mean squared error (RMSE) for estimated coefficients in the constrained fit compared to a usual unconstrained GLM for the non-negative regression (left) and non-decreasing strata (right) DGM. The x-axis corresponds to the feasibility parameter  $\gamma$ , with negative/positive values indicating unfeasible/feasible linear predictors  $\eta(x_i)$ . Positive increases in the y-axis indicate worse performances of the constrained model compared to the unconstrained, and negative changes better performances. In the first DGM (left), the ‘main’ coefficient is  $\beta_1$  and ‘covariate’ is  $\beta_2$ , while in the second (right) strata 1, 3 and 5 respectively correspond to  $\beta_1$ ,  $\beta_3$  and  $\beta_5$  in Table 1.

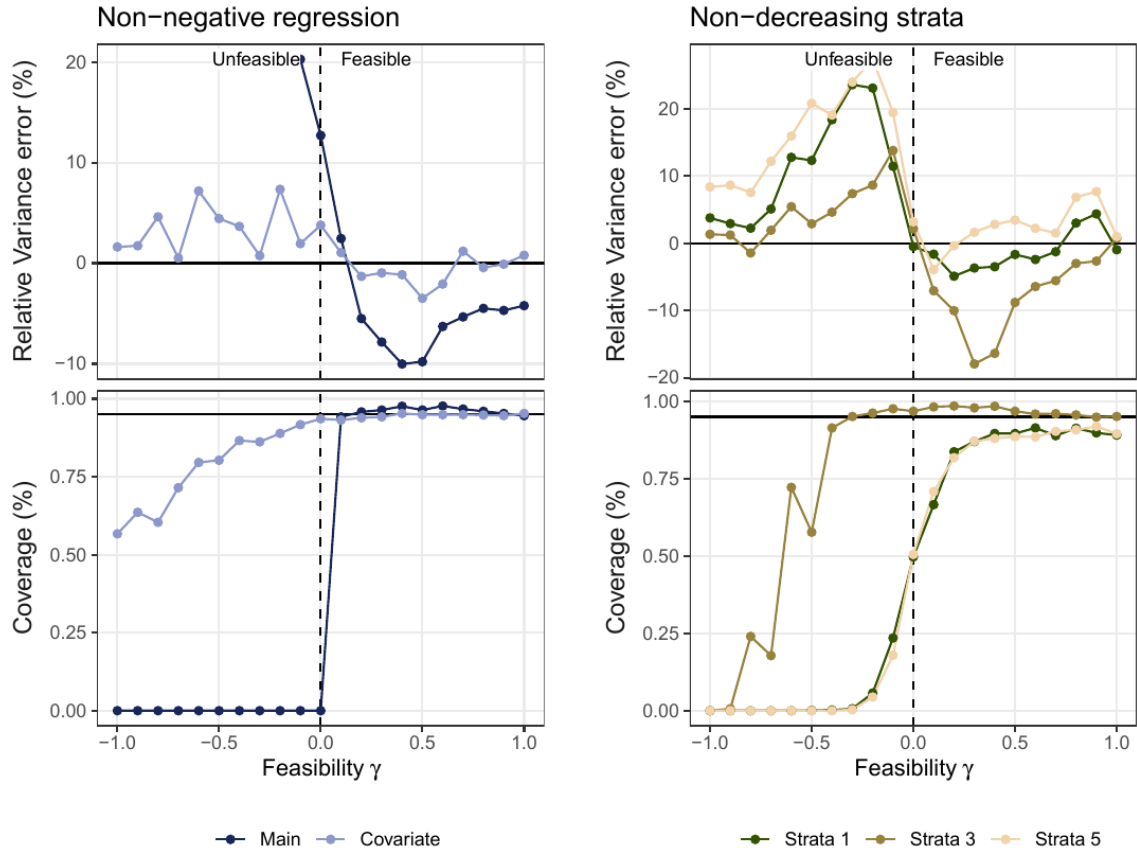


Figure 2. Evaluation of the inference procedure in a constrained GLM versus the feasibility parameter  $\gamma$ . The top row shows the Relative Variance error, *i.e.* the ratio between the average coefficient standard error and the standard deviation of estimated coefficients across simulations. The bottom row shows the coverage of a 95% confidence interval.

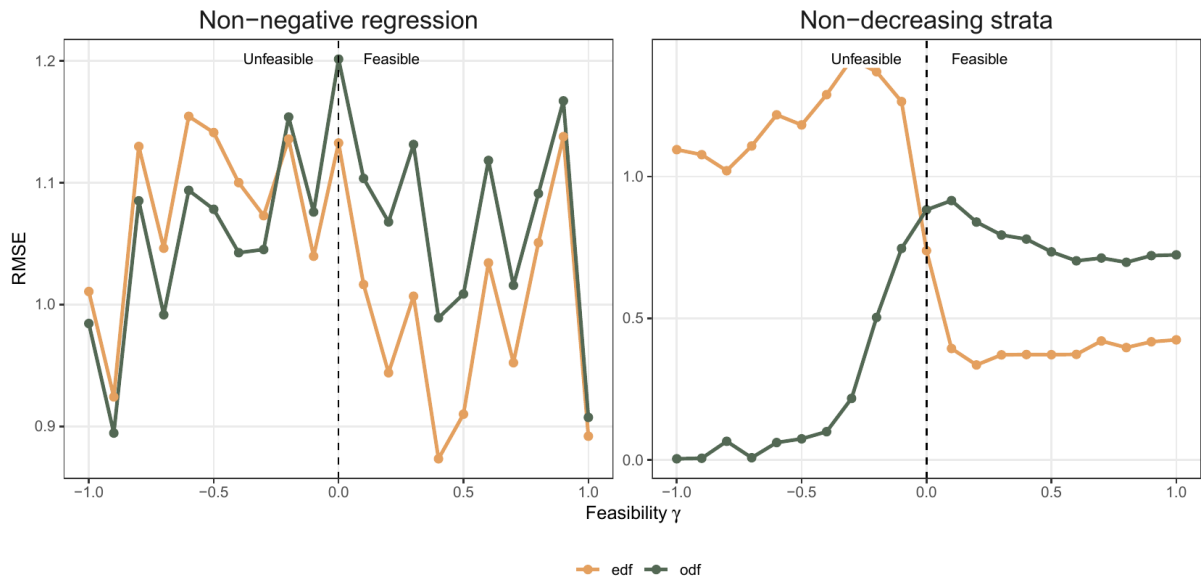


Figure 3. Average observed degrees of freedom (*odf*, in blue) across simulations and distribution of expected degrees of freedom (*edf*, in green) with the point representing the median and the segment the IQR over the  $n_{sim}$  simulations.

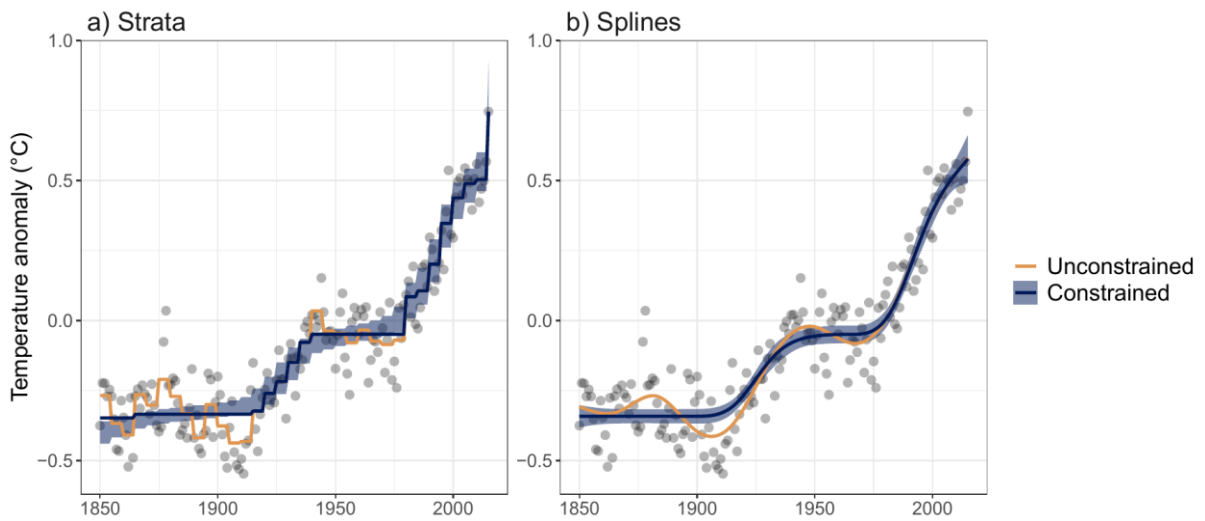


Figure 4. Annual temperature anomaly from the Global Warming data with estimated levels: a) using five-year strata as predictors and b) using natural spline bases with 10 degrees of freedom. The shaded areas represent confidence bands for the constrained model.

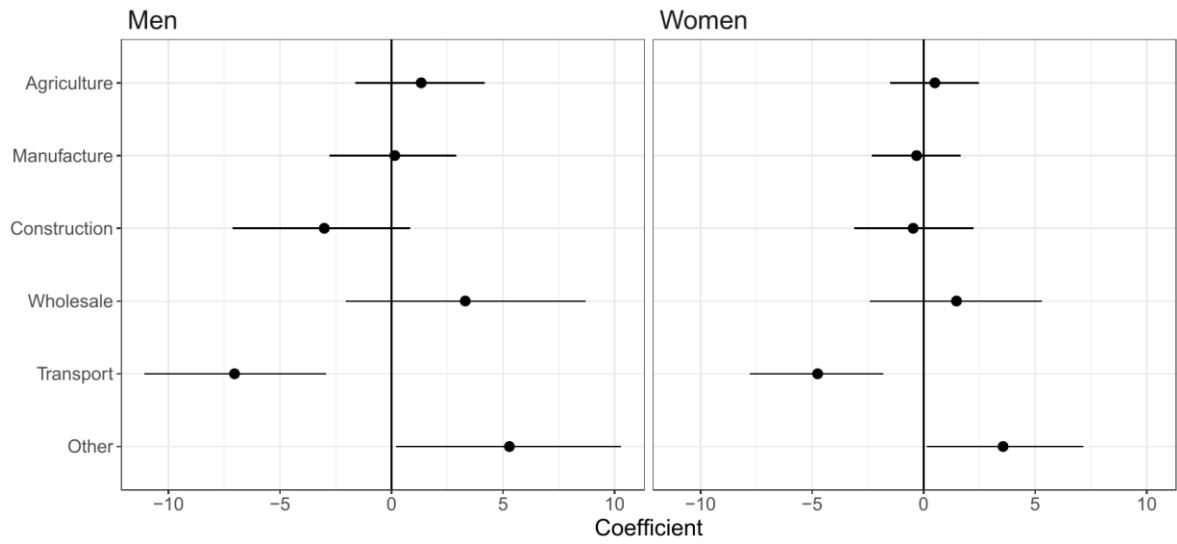


Figure 5. Estimated coefficients for the proportion of GDP each category contributes to the life expectancy of men and women across European Union member states. Horizontal lines indicate the 95% confidence interval.

## Appendix 1: Details on the CIRLS algorithm

Here, we attempt to provide some guarantees regarding the convergence of the CIRLS algorithm. We start by introducing the general class of algorithms called sequential quadratic programs (SQP) and show that CIRLS is a simplified SQP. In light of this result, we shortly discuss convergence properties of the algorithm.

### *Sequential Quadratic Programming*

Sequential Quadratic Programming (SQP) is a class of algorithms to optimise general constrained nonlinear problems. Using the notation of the main manuscript, SQPs attempt to solve

$$\begin{aligned} \min_{\boldsymbol{\beta}} f(\boldsymbol{\beta}) \\ \text{s. t. } c_i(\boldsymbol{\beta}) \geq 0 \end{aligned} \quad (9)$$

Note that the problem in equation (9) is written generally to keep notation simple, since it generally includes equality and box constraints.

To solve (9), SQP iterate the following Quadratic Program (QP) to obtain the update  $\mathbf{b}$  to  $\boldsymbol{\beta}^{[k]}$  (Boggs and Tolle, 1995; Nocedal and Wright, 2006)

$$\begin{aligned} \min_{\mathbf{b}} \left( f(\boldsymbol{\beta}^{[k]}) + \nabla f(\boldsymbol{\beta}^{[k]})^T \mathbf{b} + \frac{1}{2} \mathbf{b}^T \nabla^2 L(\boldsymbol{\beta}^{[k]}) \mathbf{b} \right) \\ \text{s. t. } \nabla c_i(\boldsymbol{\beta}^{[k]})^T \mathbf{b} + c_i(\boldsymbol{\beta}^{[k]}) \geq 0 \end{aligned} \quad (10)$$

where  $\nabla$  indicates the gradient vector and  $\nabla^2$  the Hessian evaluated at  $\boldsymbol{\beta}^{[k]}$ . The update problem (10) is a typical quadratic Taylor approximation that uses the Hessian of the Lagrangian  $L(\boldsymbol{\beta}^{[k]}) = f(\boldsymbol{\beta}^{[k]}) - \sum_i \lambda_i c_i(\boldsymbol{\beta}^{[k]})$ , where  $\lambda_i$  ( $i = 1, \dots, m$ ) are the Lagrange multipliers, to account for the constraints. The linearised constraints ensure that the updated coefficient  $\boldsymbol{\beta}^{[k+1]} = \boldsymbol{\beta}^{[k]} + \mathbf{b}$  remains feasible.

### *CIRLS as a SQP*

The CIRLS algorithm can be written as in equation (10), where  $f(\boldsymbol{\beta}^{[k]})$  is the minus log-likelihood for an exponential family evaluated at  $\boldsymbol{\beta}^{[k]}$ . First, the gradient vector of the log-likelihood can be written as

$$\nabla f(\boldsymbol{\beta}^{[k]}) = \mathbf{X}^T \mathbf{W} \mathbf{G} (\mathbf{y} - \boldsymbol{\mu}) / \phi \quad (11)$$

where  $\boldsymbol{\mu} = \mathbf{g}^{-1}(\mathbf{X}\boldsymbol{\beta}^{[k]})$  is the mean vector of  $\mathbf{y}$ ,  $\phi$  is the dispersion parameter related to the exponential family, and  $\mathbf{W}$  and  $\mathbf{G}$  are diagonal weight matrices which depend on the chosen distribution and the current coefficient value  $\boldsymbol{\beta}^{[k]}$  (Wood, 2017). Note that we drop the indices  $[k]$  from  $\mathbf{W}$  and  $\mathbf{G}$  to simplify notations.

Second, note that in our case, we only consider linear constraints  $c_i(\boldsymbol{\beta}^{[k]}) = \mathbf{c}_i^T \boldsymbol{\beta}^{[k]}$  with  $\mathbf{c}_i$  the  $i^{\text{th}}$  row of the constraint matrix  $\mathbf{C}$ . This means that their second derivative is null and that the Hessian of the Lagrangian reduces to the Hessian of the log-likelihood, i.e

$$\begin{aligned} \nabla^2 L(\boldsymbol{\beta}^{[k]}) &= \nabla^2 f(\boldsymbol{\beta}^{[k]}) - \nabla^2 \boldsymbol{\lambda} \mathbf{C} \boldsymbol{\beta}^{[k]} \\ &= \nabla^2 f(\boldsymbol{\beta}^{[k]}) \\ &= -\mathbf{X}^T \mathbf{W} \mathbf{X} / \phi \end{aligned} \quad (12)$$

where the derivation for the Hessian can be found in (Wood, 2017).

The objective function in problem (10) is minimised by a Newton step  $\mathbf{b} = \nabla^2 L(\boldsymbol{\beta}^{[k]})^{-1} \nabla f(\boldsymbol{\beta}^{[k]})$  (Boyd and Vandenberghe, 2004) and thus the updated coefficient vector is

$$\begin{aligned}
\boldsymbol{\beta}^{[k+1]} &= \boldsymbol{\beta}^{[k]} + \mathbf{b} \\
&= \boldsymbol{\beta}^{[k]} - \nabla^2 L(\boldsymbol{\beta}^{[k]})^{-1} \nabla f(\boldsymbol{\beta}) \\
&= \boldsymbol{\beta}^{[k]} + (\mathbf{XWX})^{-1} \mathbf{X}^T \mathbf{WG}(\mathbf{y} - \boldsymbol{\mu}) \\
&= (\mathbf{XWX})^{-1} \mathbf{X}^T \mathbf{WX} \boldsymbol{\beta}^{[k]} + (\mathbf{XWX})^{-1} \mathbf{X}^T \mathbf{WG}(\mathbf{y} - \boldsymbol{\mu}) \\
&= (\mathbf{XWX})^{-1} \mathbf{X}^T \mathbf{W} \{ \mathbf{G}(\mathbf{y} - \boldsymbol{\mu}) + \mathbf{X} \boldsymbol{\beta}^{[k]} \} \\
&= (\mathbf{XWX})^{-1} \mathbf{X}^T \mathbf{Wz}
\end{aligned} \tag{13}$$

which is exactly the solution of the least-square problem in the IRLS and CIRLS algorithms (equations 2 and 3 in the main manuscript).

Finally, the linearised constraint in (10) can be rewritten

$$\begin{aligned}
\nabla c_i(\boldsymbol{\beta}^{[k]})^T \mathbf{b} + c_i(\boldsymbol{\beta}^{[k]}) &= \mathbf{c}_i^T \mathbf{b} + \mathbf{c}_i^T \boldsymbol{\beta}^{[k]} \\
&= \mathbf{c}_i^T \boldsymbol{\beta}^{[k+1]}
\end{aligned} \tag{14}$$

which is obtained from the fact that the linear constraints are written  $c_i(\boldsymbol{\beta}^{[k]}) = \mathbf{c}_i^T \boldsymbol{\beta}^{[k]}$  and that the first derivative of such a constraint is simply  $\mathbf{c}_i^T$ . The resulting expression in (14) corresponds to the constraints in the quadratic program in the CIRLS algorithm.

### *Convergence properties*

SQP are generally known to converge locally even when starting relatively far from the local optimum. Specifically, in our case, both the objective function and constraints are twice differentiable, and the constraint matrix is required to be irreducible, then the conditions for local convergence are respected (Nocedal and Wright, 2006). In this case, the algorithm converges quadratically towards the local minimum, which follows from the update being a Newton step (Boggs and Tolle, 1995). This is consistent with the empirical evidence in the present paper, in which CIRLS always converges quickly to a solution.

Additionally, when using canonical link functions, the GLM log-likelihood is concave (Wedderburn, 1976), guaranteeing a unique solution. Therefore, in many instances, CIRLS will converge to a global optimum within the feasible region. This result is otherwise shown by Meyer and Woodroffe (Meyer, 2013a; Meyer and Woodroffe, 2004).

## Appendix 2: Coefficients inference

### *Distribution*

In unconstrained GLMs estimated by IRLS, the coefficient vector  $\boldsymbol{\beta}$  has distribution (Wood, 2017):

$$\widehat{\boldsymbol{\beta}}^* \sim N(\boldsymbol{\beta}^*, \phi^* \mathbf{X}^T \mathbf{W}^* \mathbf{X}) \tag{15}$$

where  $\boldsymbol{\beta}^*$ , the dispersion parameter  $\phi^*$  and weight matrix  $\mathbf{W}^*$  include the asterisk to identify them as from an unconstrained model. To get the distribution of the constrained coefficients, we first apply the affine transformation defined by the constraint matrix  $\mathbf{C}$ , and then apply the box constraints given by vectors  $\mathbf{l}$  and  $\mathbf{u}$ . This results in a Truncated Multivariate Normal (TMVN) distribution as (Horrace, 2005)

$$\mathbf{C} \widehat{\boldsymbol{\beta}} \sim \text{TMVN}(\mathbf{C} \boldsymbol{\beta}^*, \phi^* \mathbf{C} \mathbf{X}^T \mathbf{W}^* \mathbf{X} \mathbf{C}^T, \mathbf{l}, \mathbf{u}) \tag{16}$$

from which we can easily simulate (Botev, 2017; Geweke, 1991) and compute moments (Manjunath and Wilhelm, 2021).

### Back-transformation

To obtain inference for  $\widehat{\boldsymbol{\beta}}$ , one needs to transform back simulated values or moments obtained for the vector  $\mathbf{C}\widehat{\boldsymbol{\beta}}$ . However, this is not easily done if  $\mathbf{C}$  is not square, i.e. has the number of constraints  $m$  equal to the number of coefficients  $p$ . Therefore, in practice, we augment  $\mathbf{C}$  when  $m < p$  as

$$\mathbf{D} = \begin{bmatrix} \mathbf{C} \\ \mathbf{H} \end{bmatrix} \quad (17)$$

where the rows of  $\mathbf{H}$  are chosen to be orthogonal to those of  $\mathbf{C}$  and orthonormal between themselves (Tallis, 1965). A natural candidate for  $\mathbf{H}$  is therefore the null space of  $\mathbf{C}^T$ . With this augmentation, the bound vectors  $\mathbf{l}$  and  $\mathbf{u}$  then have to also be augmented as well, and we stack vectors of length  $p - m$  containing only  $-\infty$  and  $\infty$  respectively. Therefore, being uncorrelated to  $\mathbf{C}$  and unconstrained, these new variables do not influence the simulation of variables in  $\mathbf{C}\widehat{\boldsymbol{\beta}}$  and allow for easy back-transformation.

### Distributional properties

Manjunath and Wilhelm (2021) provide explicit formulas for the moments of a TMVN, which can provide information on some properties of the estimator  $\widehat{\boldsymbol{\beta}}$ . Denoting  $\boldsymbol{\theta} = \mathbf{C}\boldsymbol{\beta}^*$  as the mean vector and  $\boldsymbol{\Sigma} = \boldsymbol{\phi}^* \mathbf{C} \mathbf{X}^T \mathbf{W}^* \mathbf{X} \mathbf{C}^T$  as the covariance matrix in (4), the expectation of the  $i^{\text{th}}$  element of  $\mathbf{C}\widehat{\boldsymbol{\beta}}$  (i.e.  $\mathbf{c}_i \widehat{\boldsymbol{\beta}}$  with  $\mathbf{c}_i$  the  $i^{\text{th}}$  row of  $\mathbf{C}$ )

$$\mathbb{E}(\mathbf{c}_i \widehat{\boldsymbol{\beta}}) = \theta_i + \sum_{k=1}^m \sigma_{ik} (F_k(l_k) - F_k(u_k)) \quad (18)$$

with  $\theta_i = \mathbf{c}_i \boldsymbol{\beta}^*$ ,  $\sigma_{ik}$  the row  $i$  and column  $k$  element from the covariance matrix  $\boldsymbol{\Sigma}$ , and  $F_k(l_k)$  and  $F_k(u_k)$  the  $k^{\text{th}}$  marginal density of the TMVN (4) evaluated at its constraint bounds (as in Cartinhour, 1990). From (18), we can see that, unless  $F_k(l_k) = F_k(u_k)$  for all  $k$ , then  $\mathbb{E}(\mathbf{C}\widehat{\boldsymbol{\beta}}) \neq \boldsymbol{\theta}$  and so  $\mathbb{E}(\widehat{\boldsymbol{\beta}}) \neq \boldsymbol{\beta}^*$ . Therefore, the constraints bias the estimator  $\widehat{\boldsymbol{\beta}}$ . The formula suggests that  $\widehat{\boldsymbol{\beta}}$  is unbiased when  $F_k(l_k) = F_k(u_k)$  for all  $k$ , which happens when all  $\theta_k$  are perfectly centred between  $l_k$  and  $u_k$ , and so in the middle of the feasible region.

The covariance matrix of  $\mathbf{C}\widehat{\boldsymbol{\beta}}$  is necessarily smaller than  $\boldsymbol{\Sigma}$  since the TMVN is a contraction of a multivariate normal that concentrates the probability mass in a smaller domain. This is shown in the univariate case (Barr and Sherrill, 1999) and experimentally for the multivariate case (Manjunath and Wilhelm, 2021). The existing formula for the covariance matrix of a TMVN, although complex, shows that the variance is reduced even for untruncated variables if they are correlated with truncated ones. This suggests, for instance, that constraints would also bias and reduce the variance of confounders in epidemiological models as shown in our simulation study. However, conditional independence is preserved, meaning that the variance of untruncated variables that have null correlation with truncated ones are unaffected (Kotz et al., 2000). This fact justifies the use of the null space  $\mathbf{H}$  in (17), with the properties exposed above also being true for  $\mathbf{D}\widehat{\boldsymbol{\beta}}$ .

## Appendix 3: Additional details on the simulation study

### Generation of true coefficients

Figure SS6 shows the true coefficients generated for each value of the feasibility parameter  $\gamma$ . In the first DGM, the constraint is  $\beta_1 \geq 0$  and the generated coefficient vector is feasible for non-negative values of  $\beta_1$  (the main coefficient). The covariate coefficient ( $\beta_2$ ) is set to 1 and unconstrained, and

therefore always feasible. In the second DGM (Figure SS6b), the coefficient vector is feasible when it is increasing and unfeasible when decreasing.

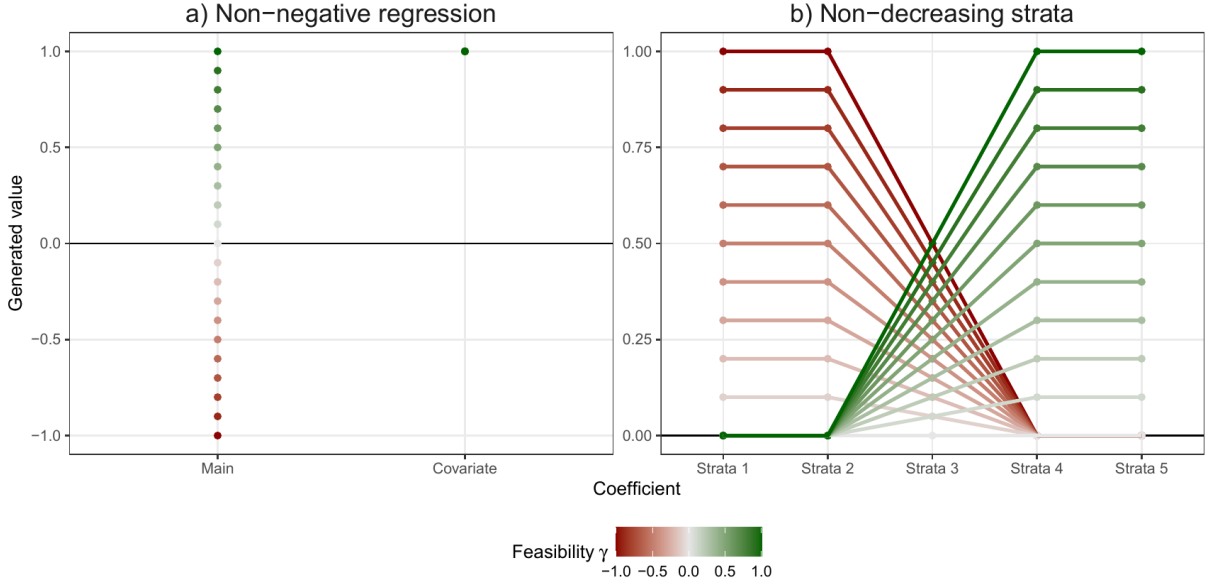


Figure S6. Generated true coefficients from both data-generating mechanisms (DGM) in the simulation study according to the feasibility parameter  $\gamma$ . Green coefficients are feasible and red are unfeasible according to the constraints, with white being on the boundary.

### Performance measures

We detail here the formulas of the performance measure reported in the main manuscript. Figure 1 of the main manuscript shows the difference in several performance measures between the constrained and unconstrained models, *i.e.* (Morris et al., 2019)

$$\begin{aligned}
 \text{Squared Bias} &= (\bar{\beta}_j - \beta_j)^2 \\
 \text{Standard Error} &= \sqrt{\frac{1}{n_{sim} - 1} \sum_b (\hat{\beta}_j^{(i)} - \bar{\beta}_j)^2} \\
 \text{RMSE} &= \sqrt{\frac{1}{n_{sim}} \sum_b (\hat{\beta}_j^{(i)} - \beta_j)^2}
 \end{aligned} \tag{19}$$

where  $\hat{\beta}_j^{(i)}$  is the estimated  $\beta_j$  for simulation  $i = 1, \dots, n_{sim}$ , and  $\bar{\beta}_j$  is the mean of the  $\hat{\beta}_j^{(i)}$ . The Squared Bias measures the systematic deviation of the estimator to the true value, the Standard Error measures the stability of the estimator across simulations, and the Root Mean Squared Error (RMSE) measures the error. Note that we have that  $RMSE^2 = \text{Squared Bias} + \text{Standard Error}^2$  and minimising the RMSE is therefore a trade-off between bias and standard error.

The performances of the uncertainty assessment are evaluated with

$$\begin{aligned}
\text{Relative Variance Error} &= \frac{n_{sim}^{-1} \sum_i \hat{V}(\hat{\beta}_j^{(i)})}{\text{Standard Error}^2} \\
\text{Coverage} &= \frac{1}{n_{sim}} \sum_i \mathbb{I}(\beta_j^{low^{(i)}} \leq \beta_j \leq \beta_j^{high^{(i)}}) \\
\text{Bias - eliminated Coverage} &= \frac{1}{n_{sim}} \sum_i \mathbb{I}(\beta_j^{low^{(i)}} \leq \bar{\beta}_j \leq \beta_j^{high^{(i)}})
\end{aligned} \tag{20}$$

with  $\hat{V}(\hat{\beta}_j^{(i)})$  the estimated variance for  $\beta_j$  from the TMVN,  $[\beta_j^{low^{(i)}}; \beta_j^{high^{(i)}}]$  is the 95% confidence intervals estimated for simulation  $i = 1, \dots, n_{sim}$ , and  $\mathbb{I}$  the indicator function. The relative variance error, therefore, represents the increase between the estimated variance and the measured variance of the estimated coefficients from the simulations. The coverage counts the proportion of confidence intervals that contain the true value of  $\beta_j$ . The bias-eliminated coverage (shown in Figure S2 below) compensates for under-coverage induced by biased estimators, using the average estimated  $\bar{\beta}_j$  as the reference instead of the true  $\beta_j$ .

Observed and expected degrees of freedom are compared to generalised degrees of freedom (Ye, 1998). These degrees of freedom are computed through the formula (Shen et al., 2004)

$$\text{Generalised degrees of freedom} = \frac{1}{\phi} \sum_{i=1}^n \text{cov}(g(\hat{\mu}_i), y_i) \tag{21}$$

where the terms are defined as in equation (1) of the main manuscript and  $\phi$  is the dispersion parameter. Formula (21) can be computed from the simulations as the  $n_{sim}$  replications allow computing the covariance for each observation and  $\phi$  is fixed by the data-generating mechanism and thus known. We then report RMSE, bias and standard error between both odf and edf, and the generalised degrees of freedom.

#### *Additional results*

Figure S7 shows the bias-eliminated coverage and shows that the bias is not the only source of coverage error when the true coefficients are not feasible. Figure S8 shows bias and standard error in the estimation of degrees of freedom using Ye's formulae as a comparison. It indicates that odf is generally unbiased but highly variable while edf can be biased for highly constrained models but less variable, explaining its lower RMSE in some instances.

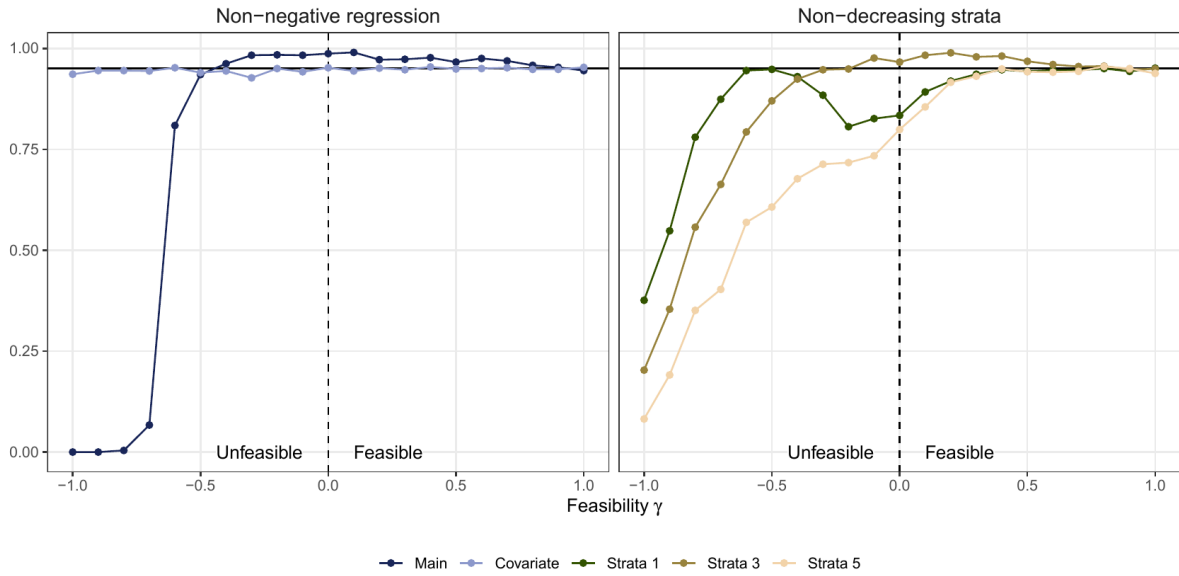


Figure S7. Bias-eliminated coverage for a 95% confidence interval in the simulation study.

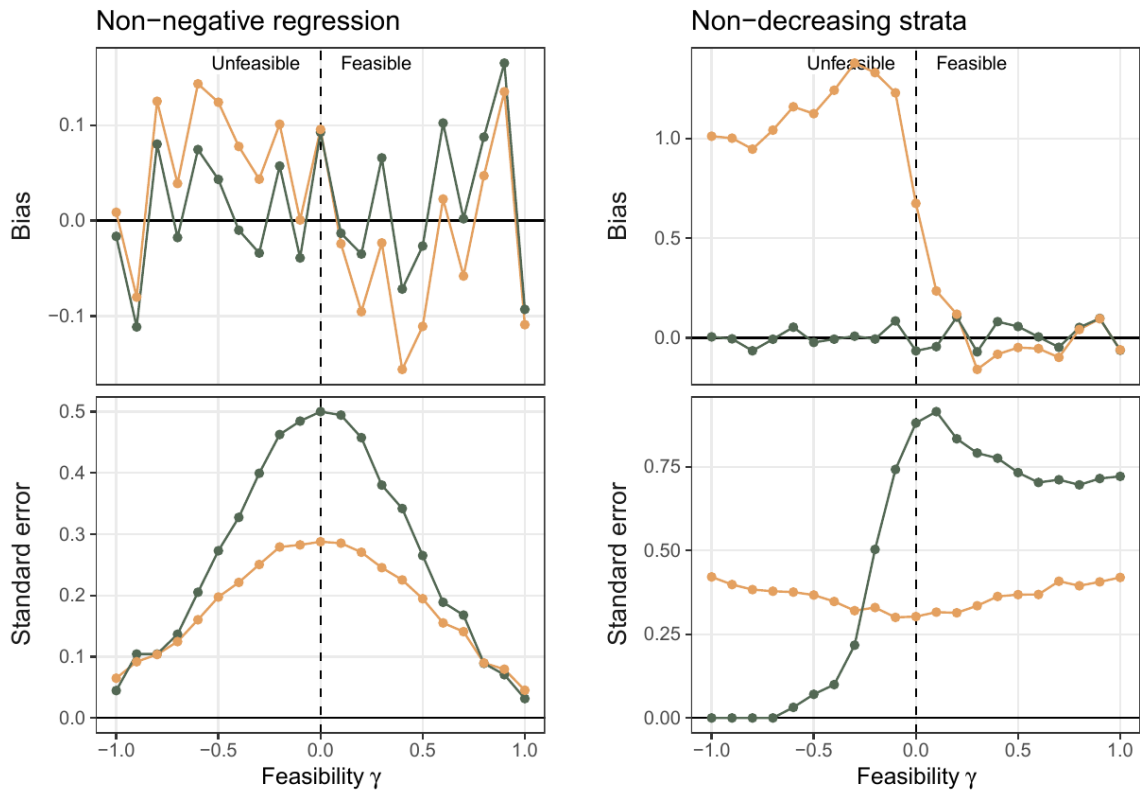


Figure S8. Bias and standard error of odf and edf in estimating simulated degrees of freedom.

## References

- Aitchison, J., Bacon-Shone, J., 1984. Log contrast models for experiments with mixtures. *Biometrika* 71, 323–330. <https://doi.org/10.1093/biomet/71.2.323>
- Akaike, H., 1974. A new look at the statistical model identification. *Autom. Control IEEE Trans. On* 19, 716–723. <https://doi.org/10.1109/tac.1974.1100705>
- Altenbuchinger, M., Rehberg, T., Zacharias, H.U., Stämmler, F., Dettmer, K., Weber, D., Hiergeist, A., Gessner, A., Holler, E., Oefner, P.J., Spang, R., 2017. Reference point insensitive molecular data analysis. *Bioinformatics* 33, 219–226. <https://doi.org/10.1093/bioinformatics/btw598>
- Alvarez, E.E., Dey, D.K., 2009. Bayesian isotonic changepoint analysis. *Ann. Inst. Stat. Math.* 61, 355–370. <https://doi.org/10.1007/s10463-007-0148-y>
- Andrews, D.W.K., 2000. Inconsistency of the Bootstrap When a Parameter is on the Boundary of the Parameter Space. *Econometrica* 68, 399–405.
- Barr, D.R., Sherrill, E.T., 1999. Mean and Variance of Truncated Normal Distributions. *Am. Stat.* 53, 357–361. <https://doi.org/10.1080/00031305.1999.10474490>
- Boggs, P.T., Tolle, J.W., 1995. Sequential Quadratic Programming. *Acta Numer.* 4, 1–51. <https://doi.org/10.1017/S0962492900002518>
- Botev, Z., Belzile [aut, L., cre, 2024. TruncatedNormal: Truncated Multivariate Normal and Student Distributions.
- Botev, Z.I., 2017. The normal law under linear restrictions: simulation and estimation via minimax tilting. *J. R. Stat. Soc. Ser. B Stat. Methodol.* 79, 125–148. <https://doi.org/10.1111/rssb.12162>
- Boyd, S., Vandenberghe, L., 2004. *Convex Optimization*, 1 edition. ed. Cambridge University Press, Cambridge, UK ; New York.
- Burnham, K.P., Anderson, D.R., 2004. Multimodel Inference: Understanding AIC and BIC in Model Selection. *Sociol. Methods Res.* 33, 261–304. <https://doi.org/10.1177/0049124104268644>
- Busing, F.M.T.A., 2022. Monotone Regression: A Simple and Fast  $O(n)$  PAVA Implementation. *J. Stat. Softw.* 102, 1–25. <https://doi.org/10.18637/jss.v102.c01>
- Cartinhour, J., 1990. One-dimensional marginal density functions of a truncated multivariate normal density function. *Commun. Stat. - Theory Methods* 19, 197–203. <https://doi.org/10.1080/03610929008830197>
- Davis, W.W., 1978. Bayesian Analysis of the Linear Model Subject to Linear Inequality Constraints. *J. Am. Stat. Assoc.* 73, 573–579. <https://doi.org/10.1080/01621459.1978.10480057>
- Dobson, A.J., Barnett, A.G., 2018. *An Introduction to Generalized Linear Models*, 4th ed. Chapman and Hall/CRC, New York. <https://doi.org/10.1201/9781315182780>
- Efron, B., Hastie, T., Johnstone, I., Tibshirani, R., 2004. Least Angle Regression. *Ann. Stat.* 32, 407–451. <https://doi.org/10.2307/3448465>
- Espinosa, J., Hennig, C., 2019. A constrained regression model for an ordinal response with ordinal predictors. *Stat. Comput.* 29, 869–890. <https://doi.org/10.1007/s11222-018-9842-2>
- Gaines, B.R., Kim, J., Zhou, H., 2018. Algorithms for Fitting the Constrained Lasso. *J. Comput. Graph. Stat.* 27, 861–871. <https://doi.org/10.1080/10618600.2018.1473777>
- Geweke, J., 1991. Efficient Simulation from the Multivariate Normal and Student-t Distributions Subject to Linear Constraints and the Evaluation of Constraint Probabilities, in: *Computing Science and Statistics. Presented at the 23rd Symposium on the Interface, Interface Foundation of North America, Fairfax, VA*, pp. 571–78.
- Geweke, J., 1986. Exact Inference in the Inequality Constrained Normal Linear Regression Model. *J. Appl. Econom.* 1, 127–141. <https://doi.org/10.1002/jae.3950010203>
- Geweke, J.F., 1996. Bayesian Inference for Linear Models Subject to Linear Inequality Constraints, in: Lee, J.C., Johnson, W.O., Zellner, A. (Eds.), *Modelling and Prediction Honoring Seymour Geisser*. Springer, New York, NY, pp. 248–263. [https://doi.org/10.1007/978-1-4612-2414-3\\_15](https://doi.org/10.1007/978-1-4612-2414-3_15)

- Ghosal, R., Ghosh, S.K., 2022. Bayesian inference for generalized linear model with linear inequality constraints. *Comput. Stat. Data Anal.* 166, 107335.  
<https://doi.org/10.1016/j.csda.2021.107335>
- Goldfarb, D., Idrani, A., 1983. A numerically stable dual method for solving strictly convex quadratic programs. *Math. Program.* 27, 1–33. <https://doi.org/10.1007/BF02591962>
- Hastie, T., Tibshirani, R., Wainwright, M., 2015. *Statistical learning with sparsity: the lasso and generalizations*. CRC Press.
- Hofner, B., Kneib, T., Hothorn, T., 2016. A unified framework of constrained regression. *Stat. Comput.* 26, 1–14. <https://doi.org/10.1007/s11222-014-9520-y>
- Horrace, W.C., 2005. Some results on the multivariate truncated normal distribution. *J. Multivar. Anal.* 94, 209–221. <https://doi.org/10.1016/j.jmva.2004.10.007>
- Hron, K., Filzmoser, P., Thompson, K., 2012. Linear regression with compositional explanatory variables. *J. Appl. Stat.* 39, 1115–1128. <https://doi.org/10.1080/02664763.2011.644268>
- Jones, P.D., Parker, D.E., Osborn, T.J., Briffa, K.R., 2000. *Global and Hemispheric Temperature Anomalies: Land and Marine Instrumental Records (1850 - 2015)*.  
<https://doi.org/10.3334/CDIAC/CLI.002>
- Kan, R., Robotti, C., 2017. On Moments of Folded and Truncated Multivariate Normal Distributions. *J. Comput. Graph. Stat.* 26, 930–934. <https://doi.org/10.1080/10618600.2017.1322092>
- Kotz, S., Balakrishnan, N., Johnson, N.L., 2000. *Continuous Multivariate Distributions, Volume 1: Models and Applications: 334*, 2nd edition. ed. Wiley-Interscience, New York.
- Lee, J.D., Sun, D.L., Sun, Y., Taylor, J.E., 2016. Exact post-selection inference, with application to the lasso. *Ann. Stat.* 44, 907–927.
- Li, J., 2025. The proximal bootstrap for constrained estimators. *J. Stat. Plan. Inference* 236, 106245.  
<https://doi.org/10.1016/j.jspi.2024.106245>
- Liew, C.K., 1976. Inequality Constrained Least-Squares Estimation. *J. Am. Stat. Assoc.* 71, 746–751.  
<https://doi.org/10.1080/01621459.1976.10481560>
- Mallows, C.L., 1973. Some Comments on CP. *Technometrics* 15, 661–675.  
<https://doi.org/10.2307/1267380>
- Manjunath, B.G., Wilhelm, S., 2021. Moments Calculation for the Doubly Truncated Multivariate Normal Density. *J. Behav. Data Sci.* 1, 17–33. <https://doi.org/10.35566/jbds/v1n1/p2>
- Masselot, P., Chebana, F., Campagna, C., Lavigne, É., Ouarda, T.B.M.J., Gosselin, P., 2023. Constrained groupwise additive index models. *Biostatistics* 24, 1066–1084.  
<https://doi.org/10.1093/biostatistics/kxac023>
- Masselot, P., Gasparrini, A., 2025. *cirls: Constrained Iteratively Reweighted Least Squares*.
- McCullagh, P., Nelder, J.A., 1989. *Generalized linear models, Monographs on Statistics and Applied Probability*.
- Meyer, M., Woodroffe, M., 2000. On the degrees of freedom in shape-restricted regression. *Ann. Stat.* 28, 1083–1104. <https://doi.org/10.1214/aos/1015956708>
- Meyer, M.C., 2018. A Framework for Estimation and Inference in Generalized Additive Models with Shape and Order Restrictions. *Stat. Sci.* 33, 595–614. <https://doi.org/10.1214/18-STS671>
- Meyer, M.C., 2013a. A Simple New Algorithm for Quadratic Programming with Applications in Statistics. *Commun. Stat. - Simul. Comput.* 42, 1126–1139.  
<https://doi.org/10.1080/03610918.2012.659820>
- Meyer, M.C., 2013b. Semi-parametric additive constrained regression. *J. Nonparametric Stat.* 25, 715–730. <https://doi.org/10.1080/10485252.2013.797577>
- Meyer, M.C., 2008. Inference using shape-restricted regression splines. *Ann. Appl. Stat.* 2, 1013–1033. <https://doi.org/10.1214/08-AOAS167>
- Meyer, M.C., 2003. A test for linear versus convex regression function using shape-restricted regression. *Biometrika* 90, 223–232. <https://doi.org/10.1093/biomet/90.1.223>

- Meyer, M.C., 1999. An extension of the mixed primal–dual bases algorithm to the case of more constraints than dimensions. *J. Stat. Plan. Inference* 81, 13–31.  
[https://doi.org/10.1016/S0378-3758\(99\)00025-7](https://doi.org/10.1016/S0378-3758(99)00025-7)
- Meyer, M.C., Woodrooffe, M., 2004. Consistent maximum likelihood estimation of a unimodal density using shape restrictions. *Can. J. Stat.* 32, 85–100. <https://doi.org/10.2307/3316001>
- Morris, T.P., White, I.R., Crowther, M.J., 2019. Using simulation studies to evaluate statistical methods. *Stat. Med.* 38, 2074–2102. <https://doi.org/10.1002/sim.8086>
- Nocedal, J., Wright, S., 2006. *Numerical Optimization*. Springer Science & Business Media.
- Oliva-Aviles, C., Meyer, M.C., Opsomer, J.D., 2019. Checking validity of monotone domain mean estimators. *Can. J. Stat.* 47, 315–331. <https://doi.org/10.1002/cjs.11496>
- Pyra, N., Wood, S.N., 2015. Shape constrained additive models. *Stat. Comput.* 25, 543–559.  
<https://doi.org/10.1007/s11222-013-9448-7>
- Sen, B., Meyer, M., 2017. Testing against a linear regression model using ideas from shape-restricted estimation. *J. R. Stat. Soc. Ser. B Stat. Methodol.* 79, 423–448.  
<https://doi.org/10.1111/rssb.12178>
- Shen, X., Huang, H.-C., Ye, J., 2004. Adaptive Model Selection and Assessment for Exponential Family Distributions. *Technometrics* 46, 306–317. <https://doi.org/10.1198/004017004000000338>
- Shi, P., Zhang, A., Li, H., 2016. Regression analysis for microbiome compositional data. *Ann. Appl. Stat.* 10, 1019–1040. <https://doi.org/10.1214/16-AOAS928>
- Silvapulle, M.J., Sen, P.K., 2005. *Constrained statistical inference: Inequality, order and shape restrictions*. John Wiley & Sons. <https://doi.org/10.1002/9781118165614>
- Stellato, B., Banjac, G., Goulart, P., Bemporad, A., Boyd, S., 2020. OSQP: an operator splitting solver for quadratic programs. *Math. Program. Comput.* 12, 637–672.  
<https://doi.org/10.1007/s12532-020-00179-2>
- Tallis, G.M., 1965. Plane Truncation in Normal Populations. *J. R. Stat. Soc. Ser. B Methodol.* 27, 301–307. <https://doi.org/10.1111/j.2517-6161.1965.tb01497.x>
- Tallis, G.M., 1961. The Moment Generating Function of the Truncated Multi-Normal Distribution. *J. R. Stat. Soc. Ser. B Methodol.* 23, 223–229. <https://doi.org/10.1111/j.2517-6161.1961.tb00408.x>
- Taylor, J., Tibshirani, R.J., 2015. Statistical learning and selective inference. *Proc. Natl. Acad. Sci.* 112, 7629–7634. <https://doi.org/10.1073/pnas.1507583112>
- Tibshirani, R., 1996. Regression Shrinkage and Selection via the Lasso. *J. R. Stat. Soc. Ser. B Methodol.* 58, 267–288. <https://doi.org/10.2307/2346178>
- Tsagris, M., 2025. Constrained least squares simplicial-simplicial regression. *Stat. Comput.* 35, 27.  
<https://doi.org/10.1007/s11222-024-10560-z>
- Wedderburn, R.W.M., 1976. On the Existence and Uniqueness of the Maximum Likelihood Estimates for Certain Generalized Linear Models. *Biometrika* 63, 27–32.  
<https://doi.org/10.2307/2335080>
- Wets, R.J.-B., 1991. Constrained estimation: Consistency and asymptotics. *Appl. Stoch. Models Data Anal.* 7, 17–32. <https://doi.org/10.1002/asm.3150070104>
- Wood, S.N., 2017. *Generalized Additive Models: An Introduction with R*, 2nd ed, Texts in Statistical Science. Chapman and Hall/CRC.
- Wu, W.B., Woodrooffe, M., Mentz, G., 2001. Isotonic regression: Another look at the changepoint problem. *Biometrika* 88, 793–804. <https://doi.org/10.1093/biomet/88.3.793>
- Ye, J., 1998. On Measuring and Correcting the Effects of Data Mining and Model Selection. *J. Am. Stat. Assoc.* 93, 120–131. <https://doi.org/10.1080/01621459.1998.10474094>
- Zhou, H., Lange, K., 2013. A Path Algorithm for Constrained Estimation. *J. Comput. Graph. Stat. Jt. Publ. Am. Stat. Assoc. Inst. Math. Stat. Interface Found. N. Am.* 22, 261–283.  
<https://doi.org/10.1080/10618600.2012.681248>

